Plasma Sources Science and Technology

Transport of negative ions across a double sheath with a virtual cathode

To cite this article: R McAdams *et al* 2011 *Plasma Sources Sci. Technol.* **20** 035023

View the article online for updates and enhancements.

Related content

- Brief Communication
  R McAdams and M Bacal
- Plasma sheath in large caesiated negative hydrogen ion sources
  D Wünderlich, R Gutser and U Fantz
- Issues in the understanding of negative ion extraction for fusion
  J P Boeuf, G Fubiani and L Garrigues

Recent citations

- Modeling of negative ion extraction from a magnetized plasma source: Derivation of scaling laws and description of the origins of aberrations in the ion beam
  G. Fubiani *et al*
- Present status of numerical modeling of hydrogen negative ion source plasmas and its comparison with experiments: Japanese activities and their collaboration with experimental groups
  A Hatayama *et al*
- Formation of stable inverse sheath in ion–ion plasma by strong negative ion emission
  Zhe Zhang *et al*

IOP ebooks™

Bringing you innovative digital publishing with leading voices to create your essential collection of books in STEM research.

Start exploring the collection - download the first chapter of every title for free.

This content was downloaded from IP address 194.81.223.66 on 25/09/2018 at 09:48

Plasma Sources Sci. Technol. **20** (2011) 035023 (13pp) doi:10.1088/0963-0252/20/3/035023

Transport of negative ions across a double sheath with a virtual cathode

R McAdams[1], A J T Holmes[2], D B King[1] and E Surrey[1]

[1] EURATOM/CCFE Fusion Association, Culham Science Centre, Abingdon, Oxfordshire OX14 3DB, UK
[2] Marcham Scientific, Hungerford, Berkshire RG17 0LH, UK

E-mail: roy.mcadams@ccfe.ac.uk

Received 14 February 2011, in final form 11 April 2011
Published 19 May 2011
Online at stacks.iop.org/PSST/20/035023

Abstract
A one-dimensional analytical model of the sheath in a negative ion source, such as those proposed for heating and diagnostic beams on present and future fusion devices, has been developed. The model, which is collisionless, describes the transport of surface produced negative ions from a cathode, across the sheath to a plasma containing electrons, positive ions and negative ions. It accounts for the situation where the emitted flux of negative ions is greater than the space charge limit, where the electric field at the cathode is negative, and a virtual cathode is formed. It is shown that, in the presence of a virtual cathode, there is a maximum current density of negative ions that can be transported across the sheath into the plasma. Furthermore, for high rates of surface production the virtual cathode persists regardless of the negative bias applied to the cathode, so that the current density transported across the sheath is limited. This is a significant observation and implies that present negative ion sources may not be exploiting all of the surface production available. The model is used to calculate the transported negative ion flux in a number of examples. The limitations of the model and proposed future work are also discussed.

1. Introduction

Future large magnetic fusion machines such as ITER will use hydrogenic neutral beams for heating, current drive and diagnostics. Due to the size of these machines and the plasma density, high energies (∼1 MeV) are required for the heating and current drive beams in order to penetrate the plasma. The neutralization efficiency of negative ions is much higher than for positive ions at these energies and so negative ion beams will be used to produce the neutral beams. For example, on ITER [1], each heating beam will be derived from a 40 A D^- beam at an extracted current density of 290 A m^{-2} to produce 16.7 MW of neutral beam power and the diagnostic beam at 100 keV requires an extracted H^- current density of 350 A m^{-2} for a 60 A beam delivering 3.3 MW of neutral beam power.

Conventional plasma ('volume') sources of negative ions can produce current densities in the range 50–200 A m^{-2} [2–4], by dissociative attachment of low energy electrons to vibrationally excited molecules, i.e. current densities lower than that required for ITER. In order to meet the higher current density requirement for ITER caesium will be injected into the volume negative ion source. The addition of caesium produces an enhancement of the negative ion current density, with reported enhancement factors in the extracted beam current in the range 2–8 [3–6]. This enhancement is thought to be due predominantly to the impingement of hydrogen atoms on the caesiated walls of the ion source leading to surface production of negative ions. The caesium reduces the work function of the surface and increases the probability of electron attachment to the hydrogen atom, i.e. the hydrogen atom is reflected off the wall as a negative ion [7]. This process also occurs for positive ions but to a lesser degree due to the fluxes involved. Current densities of 230 A m^{-2} of D^- and 340 A m^{-2} of H^- have been demonstrated [4, 8].

The negative ions created at the caesiated wall will cross back across the sheath into the plasma. In principle, the flux of negative ions produced at the wall can be increased by increasing the flux of atoms or positive ions arriving at the wall. The transported flux of negative ions depends on the potential between the wall and the plasma and the densities in the sheath of electrons, positive ions and negative ions arising from the plasma. This situation has been analysed by Wünderlich *et al* [9] using a 1D3V (one spatial co-ordinate and three velocity co-ordinates) PIC code. The model included

 © 2011 IOP Publishing Ltd Printed in the UK & the USA

both the sheath and the bulk plasma (although with no volume negative ion production). It was found that as the hydrogen atom flux at the wall was increased, the negative ion flux transported back across the sheath also increased initially and the field at the wall decreased. At a sufficiently high flux of hydrogen atoms a virtual cathode formed in the sheath and the space charge conditions in the sheath were unable to support the transport of all the negative ions produced at the wall. This virtual cathode represents a potential barrier to negative ions leaving the wall and only those with sufficient energy can reach the potential minimum of the virtual cathode and be transported to the plasma. Thus as the hydrogen atom flux increases further the transported flux stays relatively constant. This formation of the virtual cathode could then act as a limiting factor on the ion source performance. The simulations [9] show that the virtual cathode is formed at plasma parameters and atomic hydrogen densities typically found in negative ion sources.

The emission of negatively charged particles from a cathode into the sheath formed by a plasma containing positive ions, electrons and negative ions has also been analysed by Amemiya *et al* [10]. In this case the emitted particles were electrons. The model solved the 1D Poisson equation in the region between the wall and the sheath edge but did not consider the bulk plasma. This model is only valid up to the point where the electric field at the cathode is zero, i.e. the space charge limited condition. By replacing the electrons emitted from the cathode with negative ions, McAdams and Bacal [11] showed that this model gives good agreement with the 1D3V PIC code [9] in determining the negative ion flux transported across the sheath before the formation of the virtual cathode and the negative ion and positive ion fluxes at the formation of the virtual cathode.

The PIC code calculations have now been extended to two dimensions and include the effects of an extraction aperture and accelerating field together with the magnetic fields associated with the source filter field and electron deflection field in the accelerator [12, 13]. In the work of Hatayama [12] and of Taccogna *et al* [13] the virtual cathode is clearly formed under the plasma conditions studied. Importantly, in the study by Taccogna *et al* [13] it was shown that ∼91% of the surface produced negative ions were reflected by the virtual cathode and thus the extracted negative ion current was dominated by the volume produced negative ions. Only those surface produced negative ions formed very close to the extraction aperture could be extracted due the influence of an electric field parallel to the plasma grid. It was then concluded that there must be another volume production process associated with caesium to account for the measured current densities. This was also proposed earlier by McAdams and Surrey [14] based on the enhancement of the negative ion current with caesium at plasma grid bias voltages higher than the plasma potential such that no negative ions should be able to leave the surface.

Thus understanding the sheath physics is very important for understanding the production of negative ions and the source physics. The aim of this paper is to extend the model of Amemiya *et al* [10, 11] to take account of the formation of the virtual cathode. This straightforward extension illuminates the physics of the sheath due to its analytical nature and the numerical solutions required take less than 1 min on a UNIX workstation. The results allow comparison with the 1D3V PIC code simulations over the full range of emitted negative ion fluxes. The model is then applied to a range of bias potentials of the wall relative to the plasma and allows comparison with experimental results. The effect of changing the negative ion density in the plasma is also investigated. A description of the plasma and sheath is given in section 2 and the model is then described in section 3. Section 4 describes the comparison of the results from the model with the PIC code simulations and experimental results. In section 5 the proposed direction of future work is discussed.

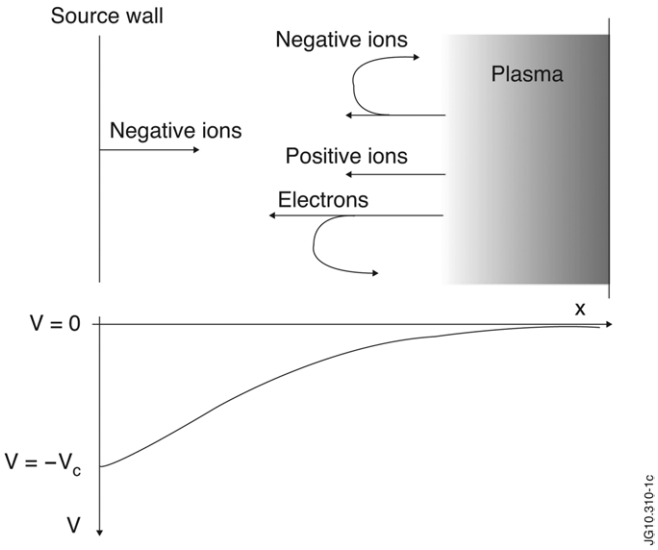

Figure 1. The plasma and sheath in the absence of a virtual cathode.

2. The plasma, the sheath and the formation of a virtual cathode

Figure 1 shows the situation with the plasma sheath and wall in the case where there is no virtual cathode. The plasma consists of positive ions, electrons and negative ions. The sheath edge is chosen to be at zero potential. The wall is then chosen to be at a potential $-V_c$. The wall acts as a cathode producing negative ions which are accelerated across the sheath. Similarly the positive ions are accelerated from the plasma to the wall. The electrons and negative ions have finite temperatures and this thermal energy means that these species can penetrate into the sheath. Those electrons and negative ions with sufficient energy to overcome the potential barrier reach the cathode and the rest are reflected back to the plasma.

The electric field at the wall is initially positive and as the flux of negative ions produced at the wall increases from zero, the field at the cathode starts to decrease. At a particular value of the negative ion flux the field will reach a value of zero. This is the familiar Child–Langmuir limit, i.e. the space charge limited condition. Further increases in the negative ion flux produced at the wall will then lead to the formation of a virtual cathode. This is how the sheath accommodates the additional space charge that cannot be transported across the

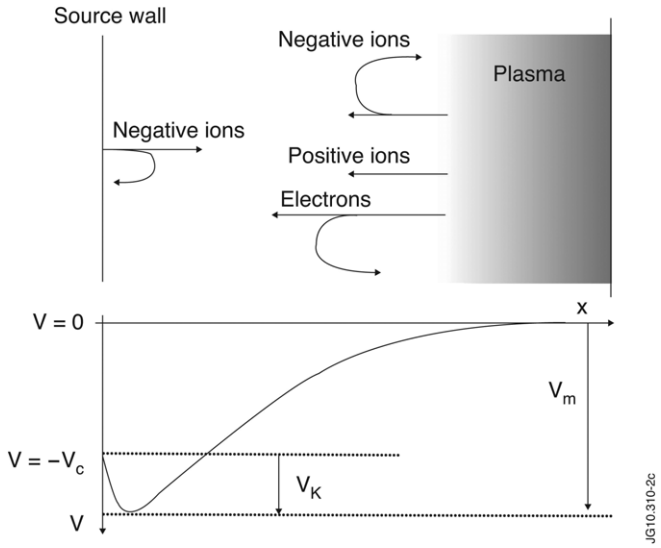

Figure 2. The plasma sheath with a virtual cathode.

sheath to the plasma. The virtual cathode in the sheath is shown in figure 2. It has a depth of V_k relative to the wall potential and the potential minimum in the sheath is at $-V_m$ relative to the plasma.

The virtual cathode retards negative ions that leave the wall unless they have sufficient energy to reach the potential minimum and are then accelerated across the sheath. Once the positive ions reach the potential minimum they are retarded by the virtual cathode before reaching the wall. Any electrons or negative ions that reach the potential minimum will then be accelerated to the wall.

There are three requirements for a virtual cathode to exist. Firstly the current density from the cathode must exceed the space charge limit as described above. Secondly the particles must be emitted with a finite energy (which also alters the space charge limit) and lastly there must be a distribution of initial energies so as to avoid an infinity in space charge density somewhere in the sheath. (If the emitted negative ions were mono-energetic the velocity could drop to zero in the virtual cathode producing an infinite density due to conservation of flux).

In reality, negative ions produced at the surface will indeed have a distribution of energies. The atoms (or positive ions) reflected as negative ions have an initial energy related to their incident energy by an energy reflection coefficient [15]. The minimum work function, W, of a caesiated surface is ~1.5 eV and the electron affinity, E_A, of the hydrogen atom is 0.75 eV. Only those atoms or ions with energy greater than a threshold energy $E_{thr} = W - E_A = 0.75$ eV can form negative ions [15]. Thus for a Maxwellian distribution of the atomic hydrogen, with temperature T_H the average energy $\langle E_{H^-} \rangle$ of the reflected negative ions is given by

$$\langle E_{H^-} \rangle = \frac{R_E \int_{E_{thr}}^{\infty} E^{1/2}(E - E_{thr}) \exp(-(E/T_H))\, dE}{\int_{E_{thr}}^{\infty} E^{1/2} \exp(-(E/T_H))\, dE} = R_E \left(\frac{\int_{E_{thr}}^{\infty} E^{3/2} \exp(-(E/T_H))\, dE}{\int_{E_{thr}}^{\infty} E^{1/2} \exp(-(E/T_H))\, dE} - E_{thr} \right) \quad (1)$$

where R_E is the energy reflection coefficient which is assumed, for simplicity, to be independent of energy and has a value of ~0.7 [15]. The denominator gives the fraction of particles with energy greater than E_{thr}. For an atomic hydrogen temperature of 0.8 eV this average energy is 0.7 eV. There is experimental evidence that the negative ions are formed with a Maxwellian distribution with a temperature equal to that of the incident atoms [16]. In that case the average energy would be $3R_E T_H/2 = 0.84$ eV which is slightly higher than the value calculated above.

The production rate of negative ions at the surface can also be calculated. The flux of hydrogen atoms at the wall, Γ_H, is

$$\Gamma_H = \frac{1}{4} n_H \sqrt{\frac{8eT_H}{M_H \pi}} \quad (2)$$

where n_H is the atomic hydrogen density, M_H the mass and e the electronic charge. Thus the current density of negative ions produced at the surface, j_{H^-}, is

$$j_{H^-} = eY(T_H)\Gamma_H \quad (3)$$

where $Y(T_H)$ is the negative ion yield for a Maxwellian distribution with temperature T_H. Wünderlich *et al* [9] in their simulations use an atomic temperature of 0.8 eV and from the results of Lee and Seidl [17] $Y(T_H)$ is ~0.12 at this atomic temperature. For a typical atomic hydrogen density of 10^{19} m^{-3} these values then give a current density of negative ions produced at the surface of ~670 A m^{-2}. In the simulations [9], with a plasma positive ion density of 4×10^{17} m^{-3} and an electron temperature of 2 eV [9], at this emission current density the virtual cathode has formed.

3. The sheath model

The formulation of the sheath model is divided into two parts. In the first part, the situation is considered up to the point where the emitted current density of negative ions is sufficient to reduce the electric field at the cathode equal to zero. This is the space charge limited condition and the emitted current at this point is the highest it can be before the formation of a virtual cathode. In this situation the analysis essentially follows that of Amemiya *et al* [10, 11] although the initial energy of the negative ions will be accounted for. This is a necessary step since the formation of a virtual cathode, as pointed out above, requires finite energy negative ions from the cathode. In accordance with the terminology of [10], the flux of negative ions from the surface will be referred to as a 'beam', to distinguish it from the flux of plasma negative ions; this is not to be confused with the *extracted* beam that is accelerated. In the second part of the model formulation, the emitted current density is higher than that supported at the space charge limited condition and a virtual cathode has formed. In the region between the minimum of the potential in the virtual cathode and the plasma the formulation is very similar to that given in the first part at the space charge limited condition since at the potential minimum the electric field must be zero. The 1D Poisson equation is then formulated for the

region between the potential minimum in the virtual cathode and the cathode. This allows the fraction of emitted negative ions reaching the virtual cathode to be calculated and these are then transported to the plasma. The equations describing these two regions are solved consistently, through the depth of the virtual cathode, and this then allows the negative ion flux transported across the sheath to be calculated along with the potential through the sheath. The sheath is considered collisionless since the Debye length ($\sim\mu$m) is much shorter than any mean free path ($\sim$cm).

3.1. The sheath before the formation of a virtual cathode

The sheath is as shown in figure 1. The densities of the plasma positive ions, electrons and negative ions at the sheath edge are n_{i0}, n_{e0} and n_{n0} with temperatures T_i, T_e and T_n, respectively. In the sheath, the densities of the positive ions, electrons and negative ions from the plasma are n_i, n_e and n_n. The potential at the sheath edge is taken to be $V = 0$ and the cathode (wall) is at a potential $-V_c$ relative to the plasma. The positive ions arrive at the sheath edge from the plasma with an initial energy eV_0, thus the density of positive ions in the sheath is given by

$$n_i = n_{i0}\left(\frac{V_0}{V_0 - V}\right)^{1/2} \tag{4}$$

where V is measured from the sheath edge and is a negative quantity. The initial energy of the positive ions is assumed to comprise of the potential difference between the plasma and the sheath edge U_0 and a thermal energy $T_i/2$. This thermal energy is that for any species with a Maxwellian distribution moving with one degree of freedom. Thus

$$V_0 = U_0 + T_i/2. \tag{5}$$

The current density of negative ions from the cathode is j_b with density n_b and the initial energy of the negative ions is eU_b. The velocity of the negative ions is v_b and their mass is M_b and the density in the sheath of the negative ions from the cathode is then given by

$$n_b = \frac{j_b}{ev_b} = \frac{j_b}{e(2e[V_c + U_b + V]/M_b)^{1/2}}. \tag{6}$$

As shown in equation (1), the energy distribution of the negative ions emitted at the surface resembles a truncated Maxwellian where the low energy particles ($E < R_E E_{thr}$) are not present. This is complicated to represent and so in order to make the mathematics tractable while allowing the physical meaning of the solution to be clear, the negative ions emitted from the surface will be assumed to have a temperature T_b and so

$$U_b = T_b/2 \tag{7}$$

U_b is effectively $\langle E_{H^-}\rangle$ as given in equation (1).

The electrons and negative ions from the plasma penetrate the sheath and are retarded and so a Boltzmann distribution is adopted for these particles:

$$n_e = n_{e0}\exp\left(\frac{V}{T_e}\right) \tag{8}$$

$$n_n = n_{n0}\exp\left(\frac{V}{T_n}\right) \tag{9}$$

where V is a negative quantity.

The one-dimensional Poisson equation for the potential in the sheath can then be written using the densities given above as

$$-\frac{d^2V}{dx^2} = \frac{e}{\varepsilon_0}\left[n_{i0}\left(1 - \frac{V}{V_0}\right)^{-\frac{1}{2}} - \frac{j_b}{e}\left(\frac{M_b}{2e}\right)^{\frac{1}{2}}(V_c + U_b + V)^{-\frac{1}{2}} - n_{e0}\exp\left(\frac{V}{T_e}\right) - n_{n0}\exp\left(\frac{V}{T_n}\right)\right] \tag{10}$$

where ε_0 is the vacuum permittivity. This equation is written in terms of the potential as measured from the sheath edge which is at infinite distance from the cathode which makes a numerical solution difficult. To overcome this, the potential is chosen to be measured from the cathode and is defined as

$$\phi = V_c + V$$

which at the cathode where $V = -V_c$ gives $\phi = 0$.

The first integration of the Poisson equation can then be carried out to give

$$\frac{\varepsilon_0}{2e}\left[\left(\frac{d\phi}{dx}\right)^2 + C\right] = 2n_{i0}V_0\left(\left(1 - \frac{(\phi - V_c)}{V_0}\right)^{1/2}\right) - \frac{2j_b}{e}\left(\frac{M_b}{2e}\right)^{1/2}[-(U_b + \phi)^{1/2}] + n_{e0}T_e\left(\exp\left(\frac{\phi - V_c}{T_e}\right)\right) + n_{n0}T_n\left(\exp\left(\frac{\phi - V_c}{T_n}\right)\right). \tag{11}$$

The constant of integration, C, can be found from the requirement that the electric field is zero at the sheath edge, i.e. when $\phi = V_c$, i.e.

$$\frac{\varepsilon_0}{2e}C = 2n_{i0}V_0 - \frac{2j_b}{e}\left(\frac{M_b}{2e}\right)^{1/2}[-(U_b + V_c)^{1/2}] + n_{e0}T_e + n_{n0}T_n.$$

Hence

$$\frac{\varepsilon_0}{2e}\left(\frac{d\phi}{dx}\right)^2 = 2n_{i0}V_0\left(\left(1 - \frac{(\phi - V_c)}{V_0}\right)^{1/2} - 1\right) + n_{e0}T_e\left(\exp\left(\frac{\phi - V_c}{T_e}\right) - 1\right) - \frac{2j_b}{e}\left(\frac{M_b}{2e}\right)^{1/2}[(V_c + U_b)^{1/2} - (U_b + \phi)^{1/2}] + n_{n0}T_n\left(\exp\left(\frac{\phi - V_c}{T_n}\right) - 1\right). \tag{12}$$

The procedure used by Amemiya *et al* [10] is used to derive boundary criteria. The plasma must be quasi-neutral at the sheath edge where $\phi = V_c$, i.e.

$$n_{i0} = n_b + n_{e0} + n_{n0}$$

and so substituting for n_b from equation (6) gives

$$n_{i0} = \frac{j_b}{e}\left(\frac{M_b}{2e}\right)^{1/2}(V_c + U_b)^{-1/2} + n_{e0} + n_{n0}. \tag{13}$$

There is also the requirement that the derivative of the total net charge density with respect to the potential is zero at the sheath edge. This then leads to an expression for the initial kinetic energy of the positive ions at the sheath edge:

$$V_0 = \frac{n_{i0}}{2\left(\dfrac{n_{e0}}{T_e} + \dfrac{n_{n0}}{T_n} - \dfrac{j_b}{e}\left(\dfrac{M_b}{e}\right)^{1/2}(2V_c + 2U_b)^{-3/2}\right)}. \tag{14}$$

The effect of the negative ions in the plasma is to decrease V_0 whereas the presence of the beam from the cathode increases V_0. In the case of no emission from the plasma but with negative ions present in the plasma then this reduces to the results of Boyd and Thompson [18] and Braithwaite and Allen [19]. For no negative ions in the plasma and for no emission from the cathode this reduces to the Bohm energy $T_e/2$.

The space charge limited current density, $j_{b\,max}$, from the cathode can also be calculated. This is the maximum current density before the formation of a virtual cathode. This condition occurs when the electric field at the cathode is zero. This condition leads to

$$\begin{aligned} j_{b\,max} = {} & \left[2n_{i0}V_0\left(\left(1 + \frac{V_c}{V_0}\right)^{1/2} - 1\right)\right. \\ & + n_{e0}T_e\left(\exp\left(\frac{-V_c}{T_e}\right) - 1\right) \\ & \left. + n_{n0}T_n\left(\exp\left(\frac{-V_c}{T_n}\right) - 1\right)\right] \\ & \times\left[\frac{2}{e}\left(\frac{M_b}{2e}\right)^{1/2}[(V_c + U_b)^{1/2} - U_b^{1/2}]\right]^{-1}. \end{aligned} \tag{15}$$

Thus up to the point where the virtual cathode is formed the sheath equations can be solved as follows. The densities of the electrons and the negative ions are given along with their temperatures and the other parameters such as the plasma potential and the initial energy of the negative ions from the cathode. By substituting equation (13) for the positive ion density and equation (14) for the initial energy of the positive ions into equation (15) an expression is obtained for the maximum current density before the virtual cathode is formed. This expression is of the form $j_{b\,max} = f(j_{b\,max})$ where the solution is a fixed value of the function f. This can be solved straightforwardly by iterative methods. Having obtained $j_{b\,max}$, the positive ion density can be obtained from equation (13) and this leads to a value for the initial positive ion energy given by equation (14). Now the differential equation for the potential, equation (12), can be integrated numerically to give the potential through the sheath.

McAdams and Bacal [11] calculated both $j_{b\,max}$ and the positive ion flux across the sheath for the plasma conditions used in the simulations of Wünderlich *et al* [9] and found good agreement with those simulations. This is to be expected since the simulations must solve, albeit in a different manner, the Poisson equation in the sheath.

3.2. The sheath between the minimum potential of the virtual cathode and the plasma

The potential is a minimum at the virtual cathode. The virtual cathode, as shown in figure 2, has a depth V_k relative to the cathode and the relationship between the potentials is

$$V_m = V_c + V_k. \tag{16}$$

Furthermore the electric field is zero at the potential minimum otherwise it would not be continuous. Since the electric field is zero, this corresponds to the space charge limited condition in the case where no virtual cathode has been formed as discussed in section 3.1, as if the emitting surface had been moved to the potential minimum. Thus the flux of negative ions transported from this point to the plasma is the space charge limited current given by equation (15) but with the potential V_c now replaced by the potential between the plasma and the potential minimum, V_m, i.e.

$$\begin{aligned} j_{b\,max} = {} & \left[2n_{i0}V_0\left(\left(1 + \frac{V_m}{V_0}\right)^{1/2} - 1\right)\right. \\ & + n_{e0}T_e\left(\exp\left(\frac{-V_m}{T_e}\right) - 1\right) \\ & \left. + n_{n0}T_n\left(\exp\left(\frac{-V_m}{T_n}\right) - 1\right)\right] \\ & \times\left[\frac{2}{e}\left(\frac{M_b}{2e}\right)^{1/2}[(V_m + U_b)^{1/2} - U_b^{1/2}]\right]^{-1}. \end{aligned} \tag{17}$$

There is a very important point in applying equation (15) to describe the flux transported from the minimum of the virtual cathode as expressed in equation (17). In moving from the cathode to the minimum of the virtual cathode the negative ions have been retarded by the potential V_k. Only those with an energy greater than eV_k will reach the virtual cathode. However in equation (17) the same initial energy, U_b, is used for the negative ions at the virtual cathode as at the cathode. The average energy of a Maxwellian distribution moving through a retarding sheath remains constant. The energy of those negative ions reaching the potential minimum is reduced but so is the number of negative ions reaching this point and so the average energy remains the same. This result is proved in the appendix.

In order to solve equation (17) the value of V_k must be known. Since, for a consistent solution, the flux of negative ions from the cathode that reaches the virtual cathode must also be $j_{b\,max}$, V_k can be found by solving equation (17) with the equations describing the flux of negative ions reaching the virtual cathode. This is discussed in the next section.

The potential in the region between the virtual cathode and the plasma can then be found by integrating equation (12)

with V_c replaced by V_m subject to the boundary conditions $d\phi/dx = 0$ at $\phi = 0$. These boundary conditions where the field and potential are both zero at the starting point make solutions such as fourth order Runge–Kutta difficult to start. To overcome this an initial starting point is found by expanding in ϕ such that for very small values of ϕ

$$\frac{\varepsilon_0}{2e}\left(\frac{d\phi}{dx}\right)^2 = \phi \times \left(\frac{j_{b\,max}}{e}\left(\frac{M_b}{eT_b}\right)^{1/2} - \frac{n_{i0}}{(1+(V_m/V_0))^{1/2}} + n_{e0}\exp\left(-\frac{V_m}{T_e}\right) + n_{n0}\exp\left(-\frac{V_m}{T_n}\right)\right) \tag{18}$$

or

$$\left(\frac{d\phi}{dx}\right)^2 = H\phi$$

which has the solution

$$\phi = \frac{Hx^2}{4}. \tag{19}$$

This allows the potential to be calculated at an initial value of x from the potential minimum and to start the numerical integration to give the potential to the plasma.

3.3. The sheath between the cathode and the minimum potential of the virtual cathode

The field at the virtual cathode is zero and thus as shown in section 3.2, the transported negative ion flux to the plasma is $j_{b\,max}$ as given in equation (17). This value of $j_{b\,max}$ is the fraction of the emitted flux j_b from the cathode that reaches the potential minimum, i.e.

$$j_{b\,max} = j_b \exp\left(-\frac{V_k}{T_b}\right). \tag{20}$$

This equation is derived in section 3.3.3. For a given emission current, using equations (20) and (17), values of $j_{b\,max}$ and V_k can be determined through an iterative procedure.

In order to calculate the potential between the cathode and the virtual cathode the one-dimensional Poisson equation in the region must be developed by determining the densities of the various species in this sheath region and then solved. As before we use a potential, θ, in this region defined as being zero at the potential minimum. In the sections below the densities of the various species are considered.

3.3.1. The positive ion density. The positive ion density has two forms depending on whether all the ions can reach the cathode when $\theta < V_m + U_0$ or only some of them at greater potentials. U_0 is used instead of V_0 because V_0 contains the ionic thermal element of the ion sound speed and this is not relevant when potential barriers are considered. All ions have the U_0 energy but only some of them have V_0 or more. Hence for potentials smaller than this critical potential all the positive ions reach the cathode and so using conservation of flux from the sheath edge

$$\theta < V_m + U_0 \qquad n_i = \frac{n_{i0}V_0^{1/2}}{(V_m + V_0 - \theta)^{1/2}}. \tag{21a}$$

At larger values of the potential the positive ions are retarded similarly to the electrons and negative ions from the plasma in the sheath and so a Boltzmann factor is used to describe this. Thus if j_i is the flux arriving at the critical potential then the flux, J_i, at greater potentials is given by

$$\theta > V_m + U_0 \qquad J_i = j_i \exp\left(-\frac{(\theta - V_m - U_0)}{T_i}\right) = en_{i0}\left(\frac{2eV_0}{M_i}\right)^{1/2}\exp\left(-\frac{(\theta - V_m - U_0)}{T_i}\right)$$

and so

$$n_i = \frac{J_i}{e\left(\frac{2e}{M_i}\frac{T_i}{2}\right)^{1/2}} = \frac{n_{i0}V_0^{1/2}}{(T_i/2)^{1/2}}\exp\left(-\frac{(\theta - V_m - U_0)}{T_i}\right) \tag{21b}$$

where M_i is the positive ion mass. At the critical potential $\theta = V_m + U_0$ the densities given by equations (21*a*) and (21*b*) are continuous. However, the density at the critical potential is slightly higher than the value of the sheath edge. This is because the potential energy, U_0, is considered for the changeover to the Boltzmann distribution and not the total energy V_0.

3.3.2. The electron and negative ion densities arising from the plasma. The fluxes of electrons and negative ions from the plasma that reach into the virtual sheath, j_{ev} and j_{nv}, respectively, are conserved as they are accelerated towards the cathode. The densities, n_e and n_n, of these species are found by dividing the flux by the local velocity, i.e. for electrons

$$j_{ev} = en_{e0}\left(\frac{eT_e}{m}\right)^{1/2}\exp\left(\frac{-V_m}{T_e}\right)$$

hence

$$n_e = \frac{j_{ev}}{e\left(\frac{2e}{m}\left(\theta + \frac{T_e}{2}\right)\right)^{1/2}} = n_{e0}\exp\left(\frac{-V_m}{T_e}\right) \times \left(1 + \frac{2\theta}{T_e}\right)^{-1/2} \tag{22}$$

where m is the electron mass and for the negative ions

$$j_{nv} = en_{n0}\left(\frac{eT_n}{M}\right)^{1/2}\exp\left(\frac{-V_m}{T_n}\right)$$

hence

$$n_n = \frac{j_{nv}}{e\left(\frac{2e}{M}\left(\theta + \frac{T_n}{2}\right)\right)^{1/2}} = n_{n0}\exp\left(\frac{-V_m}{T_n}\right)\left(1 + \frac{2\theta}{T_n}\right)^{-1/2} \tag{23}$$

where M is the negative ion mass.

The average energies of the electrons and negative ions at the sheath edge are $T_e/2$ and $T_n/2$, respectively. At $\theta = 0$, the potential minimum equations (8) and (9) are recovered with $V = -V_m$.

3.3.3. The negative ion density arising from the cathode. We assume that there is a thermal distribution of emitted negative ions, whose density is n_b. The density at the virtual cathode is simply

$$n_b(\theta = 0) = \frac{j_{b\,max}}{e\left(\frac{2e}{M_b}\frac{T_b}{2}\right)^{1/2}} \tag{24}$$

while at the real cathode the density is

$$n_b(\theta = V_k) = \frac{j_b}{e\left(\frac{2e}{M_b}\frac{T_b}{2}\right)^{1/2}}. \tag{25}$$

The flux of negative ions decreases from the cathode according to the equation

$$j_b(\theta) = j_b \exp\left(\frac{(\theta - V_k)}{T_b}\right). \tag{26}$$

This is consistent with equation (20) and, as explained, can be used with equation (17) to determine the negative ion flux transported across the sheath including the virtual cathode.

Combining equations (24), (25) and (26) and using the cathodic emission current, j_b, as the controlling parameter gives

$$n_b = \frac{j_b \exp\left(\frac{(\theta - V_k)}{T_b}\right)}{e\left(\frac{2e}{M_b}\frac{T_b}{2}\right)^{1/2}}. \tag{27}$$

This equation satisfies equations (24) and (25) and is consistent with a classical Boltzmann attenuation of trapped particles.

3.3.4. Solution of Poisson's equation in the virtual cathode region. Poisson's equation in the virtual cathode sheath is given by

$$\frac{\varepsilon_0}{e}\frac{d^2\theta}{dx^2} = -n_i + n_b + n_e + n_n \tag{28}$$

where the densities are given by equations (21*a*) and (21*b*) (depending if θ is less than or greater than $V_m + U_0$) and equations (22), (23) and (27). This can be integrated once to give expressions for the electric field in the virtual cathode for the two cases depending on the value of θ.

In the case where $\theta < V_m + U_0$ this gives

$$\begin{aligned}\frac{\varepsilon_0}{2e}\left[\left(\frac{d\theta}{dx}\right)^2 + B\right] &= 2n_{i0}V_0\left(1 + \frac{(V_m - \theta)}{V_0}\right)^{1/2} \\ &+ n_{e0}T_e \exp\left(\frac{-V_m}{T_e}\right)\left(1 + \frac{2\theta}{T_e}\right)^{1/2} \\ &+ \frac{j_b T_b \exp\left(\frac{(\theta - V_k)}{T_b}\right)}{e\left(\frac{eT_b}{M_b}\right)^{1/2}} \\ &+ n_{n0}T_n \exp\left(\frac{-V_m}{T_n}\right)\left(1 + \frac{2\theta}{T_n}\right)^{1/2}.\end{aligned} \tag{29}$$

The constant of integration B is found from the condition that the field $d\theta/dx$ is zero at $\theta = 0$, i.e.

$$\begin{aligned}\frac{\varepsilon_0}{2e}B &= 2n_{i0}V_0\left(1 + \frac{V_m}{V_0}\right)^{1/2} + n_{e0}T_e \exp\left(\frac{-V_m}{T_e}\right) \\ &+ n_{n0}T_n \exp\left(\frac{-V_m}{T_n}\right) + \frac{j_b T_b \exp\left(-\frac{V_k}{T_b}\right)}{e\left(\frac{eT_b}{M_b}\right)^{1/2}}.\end{aligned} \tag{30}$$

In the case where $\theta > V_m + U_0$ the first integration of the Poisson equation gives

$$\begin{aligned}&\frac{\varepsilon_0}{2e}\left[\left(\frac{d\theta}{dx}\right)^2 + B\right] \\ &= \sqrt{2}n_{i0}V_0^{1/2}T_i^{1/2}\exp\left(-\frac{(\theta - V_m - U_0)}{T_i}\right) \\ &+ n_{e0}T_e \exp\left(\frac{-V_m}{T_e}\right)\left(1 + \frac{2\theta}{T_e}\right)^{1/2} \\ &+ \frac{j_b T_b \exp\left(\frac{(\theta - V_k)}{T_b}\right)}{e\left(\frac{eT_b}{M_b}\right)^{1/2}} \\ &+ n_{n0}T_n \exp\left(\frac{-V_m}{T_n}\right)\left(1 + \frac{2\theta}{T_n}\right)^{1/2}.\end{aligned} \tag{31}$$

Note that the integration constant for the case in equation (31) is the same constant as in equation (29) and as given in equation (30). That the integration constant must be the same in the two cases arises from the requirement that the field is continuous at the value of $\theta = V_m + U_0$. Comparing the positive ion terms in equations (29) and (30) at this value of theta gives (all the other species terms are the same in the two equations) from equation (29)

$$\begin{aligned}\frac{\varepsilon_0}{2e}\left(\left(\frac{d\theta}{dz}\right)^2 + B\right) &= 2n_{i0}V_0\left(1 + \frac{(V_m - V_m - U_0)}{V_0}\right)^{1/2} \\ &+ \text{remaining terms} \\ &= 2n_{i0}V_0\left(\frac{T_b}{2V_0}\right)^{1/2} + \text{remaining terms}\end{aligned}$$

and from equation (31)

$$\begin{aligned}&\frac{\varepsilon_0}{2e}\left(\left(\frac{d\theta}{dx}\right)^2 + B\right) \\ &= \sqrt{2}n_{i0}V_0^{1/2}T_b^{1/2}\exp\left(-\frac{(V_m + U_0 - V_m - U_0)}{T_i}\right) \\ &+ \text{remaining terms} \\ &= \sqrt{2}n_{i0}V_0^{1/2}T_b^{1/2} + \text{remaining terms}.\end{aligned}$$

Thus both θ (as shown in section 3.3.1) and $d\theta/dx$ are continuous at $\theta = V_m + U_0$ if the integration constant B is the same for each case.

The potential in the virtual cathode region can be found by numerically integrating equations (29) and (31). As before, in the region between the virtual cathode and the plasma, the

potential and the field are zero at the integration starting point making a fourth order Runge–Kutta method difficult to start. A starting point may be found as before by expanding for very small values of θ to give

$$\frac{\varepsilon_0}{2e}\left(\frac{\mathrm{d}\theta}{\mathrm{d}x}\right)^2 = \theta \times \left[-n_{\mathrm{i}0}\left(\frac{1}{1+\dfrac{V_{\mathrm{m}}}{V_0}}\right)^{1/2} + n_{\mathrm{e}0}\exp\left(\frac{-V_{\mathrm{m}}}{T_{\mathrm{e}}}\right) + n_{\mathrm{n}0}\exp\left(\frac{-V_{\mathrm{m}}}{T_{\mathrm{n}}}\right) + \frac{j_{\mathrm{b}}\exp\left(-\dfrac{V_{\mathrm{k}}}{T_{\mathrm{b}}}\right)}{e\left(\dfrac{eT_{\mathrm{b}}}{M_{\mathrm{b}}}\right)^{1/2}}\right] \tag{32}$$

which can be written

$$\left(\frac{\mathrm{d}\theta}{\mathrm{d}x}\right)^2 = G\theta$$

and this has the solution

$$\theta = \frac{Gx^2}{4}. \tag{33}$$

This allows an initial starting point for the integration to be calculated in addition to $\theta = 0$, $\mathrm{d}\theta/\mathrm{d}x = 0$ at $x = 0$.

4. Applications of the sheath model

The sheath model is applied to three example cases in this section. The first example considers the case of a fixed potential difference between the plasma and the cathode and the emitted current from the cathode is varied. This effectively replicates the simulations of Wünderlich *et al* [9] and is a useful check for the model. The second example is for the case of a fixed emission current of negative ions at the cathode but the potential between the cathode and the plasma is decreased to zero. The third example considers the effect of negative ions in the plasma. The examples only cover hydrogen operation but the model can be trivially extended to deuterium.

4.1. Negative ion transport across the sheath for a fixed plasma potential

The 1D3V simulations of Wünderlich *et al* [9] studied the region between a plasma source and the plasma grid. Only negative ion production at the wall by positive ion and atomic hydrogen impingement was considered, i.e. no volume negative ion production was considered. The transmitted negative ion flux from the plasma grid was calculated as the atomic hydrogen density was increased. The virtual cathode is formed between atomic hydrogen densities of 10^{18} and $10^{19}\,\mathrm{m}^{-3}$. The formation of the virtual cathode changes the plasma conditions somewhat. From the simulations, at an atomic hydrogen density of $10^{18}\,\mathrm{m}^{-3}$ the plasma parameters, where the field is approximately zero, were [20] $n_{\mathrm{i}} \sim 3.9 \times 10^{17}\,\mathrm{m}^{-3}$, $T_{\mathrm{i}} = 0.8\,\mathrm{eV}$, $n_{\mathrm{e}} \sim 3.5 \times 10^{17}\,\mathrm{m}^{-3}$, $T_{\mathrm{e}} = 2\,\mathrm{eV}$, $V_{\mathrm{c}} = -5\,\mathrm{V}$, $T_{\mathrm{H}} = 0.8\,\mathrm{eV}$.

Applying the sheath model with these conditions gives the results shown in figure 3, where the potentials for three values

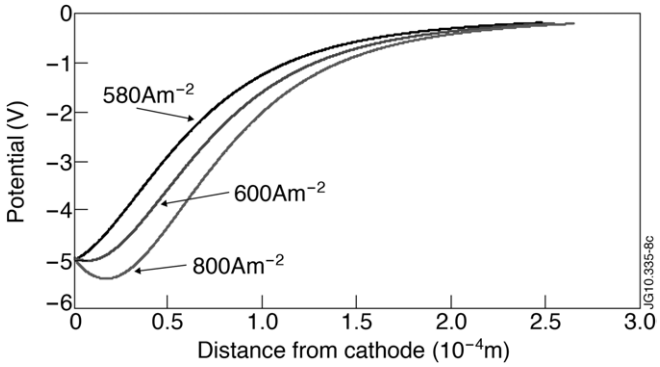

Figure 3. The sheath potentials for negative ion current densities of 580, 600 and 800 A m^{-2} at the surface. The plasma conditions are described in the text.

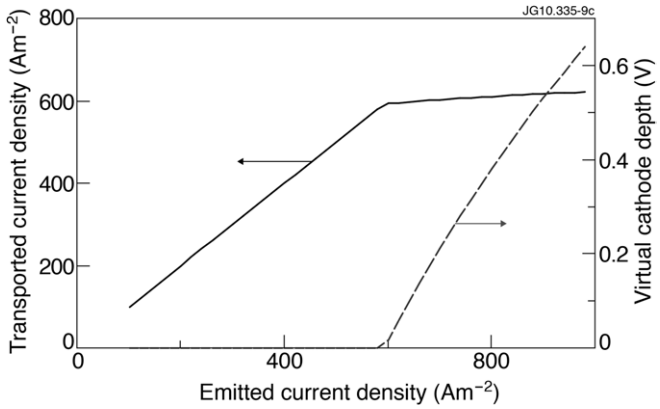

Figure 4. The dependence of the transported negative ion current density (——) and depth of the virtual cathode (----) on the emitted current density. The plasma conditions are described in the text.

of the emitted negative ion current density of 580, 600 and 800 A m^{-2} are shown. For an atomic hydrogen temperature of 0.8 eV the corresponding average energy of the negative ions leaving the plasma grid is 0.7 eV from equation (1) and thus the negative ion effective temperature T_{b} is 1.4 eV (equation (7)). Figure 3 shows at 580 A m^{-2} the virtual cathode has not formed and the electric field is positive. At 600 A m^{-2} the virtual cathode has just formed and at 800 A m^{-2} the potential minimum in the sheath is clear.

In figure 4 the transported current density across the sheath and also the depth of the virtual cathode are plotted as a function of the emitted current density. All the emitted current density is transported across the sheath until the virtual cathode is formed. The transported current density then rises slowly as the depth of the virtual cathode increases. This is the behaviour found by Wünderlich *et al* [9].

The virtual cathode is formed at an emitted current density of ~600 A m^{-2}. Using equations (2) and (3) this corresponds to an atomic hydrogen density of $\sim 1.0 \times 10^{19}\,\mathrm{m}^{-3}$ (the positive ion contribution to the surface negative ion production is relatively small). In the work of Wünderlich *et al* [9] the virtual cathode is formed between atomic hydrogen densities of 10^{18} and $10^{19}\,\mathrm{m}^{-3}$ but the transported negative ion current density starts to saturate close to $10^{19}\,\mathrm{m}^{-3}$ or a current density of ~630 A m^{-2}. This is a higher value of current density than

found in the present calculation. The calculation by McAdams and Bacal [11] using the amended model of Amemiya *et al* [10] found that the virtual cathode formed at a current density of 310 A m^{-2} which is lower than the value of Wünderlich *et al*. This discrepancy is probably due to the initial energy of the negative ions produced at the surface. In Wünderlich *et al* the negative ion initial energy is determined by the initial atomic velocity and the energy reflection coefficient. In the work of McAdams and Bacal [11] the negative ions are formed at the surface with zero energy. In the present case the initial energy is 0.7 eV. A calculation at an initial energy of 0.6 eV shows that the virtual cathode is formed at ∼565 A m^{-2}. Thus as the initial energy of the negative ion is increased the virtual cathode is formed at higher current density. This is a reflection of the well known result that the space charge current limit for acceleration between two planes increases as the initial injection energy increases (see [21] for example).

4.2. Negative ion transport across the sheath as the potential between the plasma and cathode is varied

It is common practice when accelerating a beam of negative ions to bias the plasma grid, or part of it, increasingly positive to suppress the co-extracted flux of electrons whilst having only a small effect on the extracted negative ion current. If the whole plasma grid is biased it is usually with respect to the source body. In terms of the potential between the plasma and cathode this increasing bias voltage corresponds to reducing this potential difference. This can then be expected to affect the transport of negative ions from the cathode to the plasma since there will be reduction in the voltage to support their space charge.

The effect of changing the cathode potential on the transported current density and the corresponding virtual cathode depth for current densities emitted at the surface of 600 A m^{-2} and 800 A m^{-2} are shown in figure 5(*a*) for the plasma conditions considered previously. The corresponding virtual cathode depth for these two cases is shown in figure 5(*b*).

At a current density of 600 A m^{-2} the virtual cathode is not formed under these conditions until the potential difference between the plasma and cathode is less than ∼5 V. Thus at greater potential differences there is no virtual cathode and the sheath is able to support and transport all the negative ions produced at the surface. For potential differences less than this value the sheath cannot sustain the full emission current and the virtual cathode is formed resulting is some of the negative ions being reflected back to the wall and the transported current is reduced. At the higher current density of 800 A m^{-2} the virtual cathode persists at potential differences greater than 10 V and the transmitted current is attenuated throughout the range of voltages shown in the graph.

This may seem counter-intuitive but arises from the condition that, for a real sheath solution of equation (29) or (31),

$$(\mathrm{d}\theta/\mathrm{d}x)^2 \geqslant 0$$

which defines a maximum transported negative ion flux, $j_{\mathrm{b\ max}}$, as given by equation (17). Examination of equation (17)

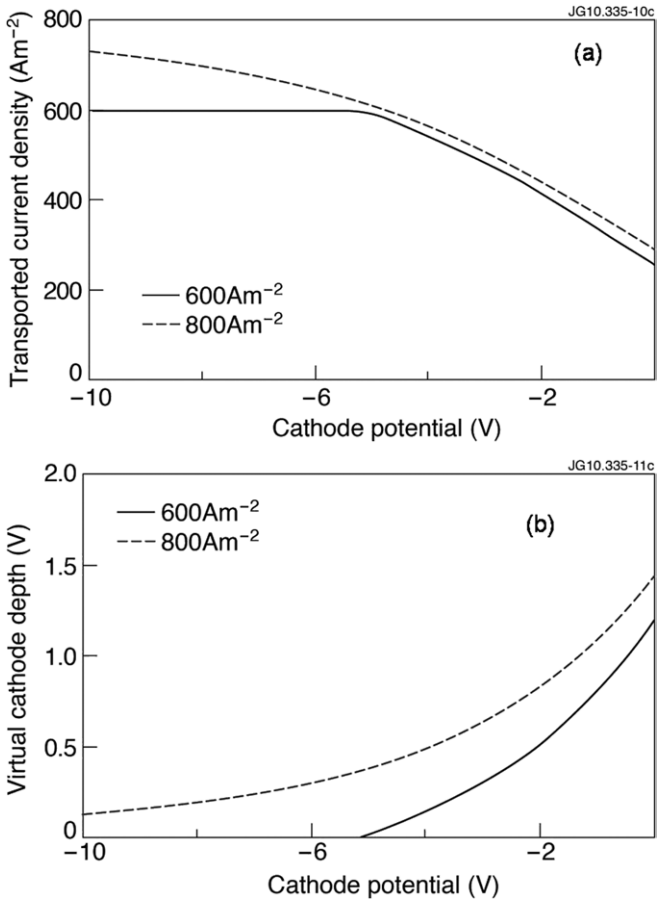

Figure 5. (*a*) The transported negative ion current density and (*b*) the virtual cathode depth as the cathode potential is varied for 600 A m^{-2} (——) and 800 A m^{-2} (----) emission at the cathode.

in the limit of large cathode potential, V_{c}, shows that $j_{\mathrm{b\ max}}$ becomes independent of V_{c} and only depends on n_{i0} and V_0, the positive ion characteristics of the plasma. Thus if the surface production rate exceeds the value of $j_{\mathrm{b\ max}}$ the virtual cathode will attenuate it and increasing the cathode negative bias will not recover the un-transported negative ions. The only remedy is to increase the positive ion density. This is an important observation with significant implications for attempts to improve present negative ion sources dominated by surface production; increasing the surface yield will not necessarily increase the negative ion density available for extraction. Indeed, increasing the negative ion density must be approached by increasing the positive ion density in the plasma and this may imply a different type of discharge is required than the rf driven plasma sources planned for ITER. Incidentally, caesium would also assist in this regard as it increases the positive ion density in the source through its presence in the plasma.

The density of the surface produced negative ions at the sheath edge, n_{b0}, is calculated according to

$$n_{\mathrm{b0}} = \frac{j}{e\sqrt{\dfrac{2e(V_{\mathrm{m}} + U_{\mathrm{b}})}{M_{\mathrm{b}}}}} \tag{34}$$

where $j = j_{\mathrm{b}}$ if a virtual cathode has not been formed and $j = j_{\mathrm{b\ max}}$ if a virtual cathode has been formed. The potential

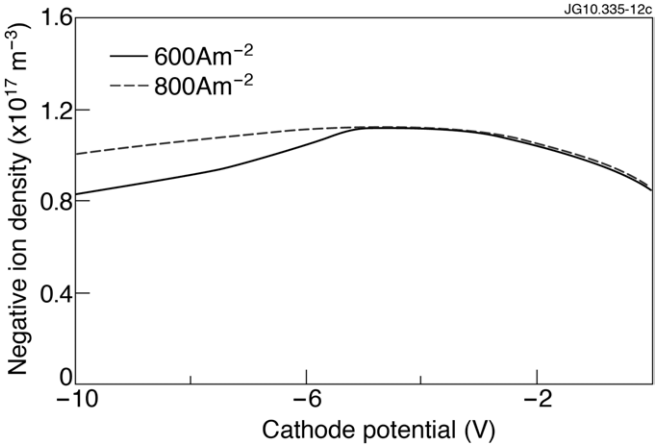

Figure 6. The negative ion density at the sheath edge as the cathode potential is varied for 600 A m^{-2} (——) and 800 A m^{-2} (----) emission at the cathode.

from the minimum of the virtual cathode to the plasma, V_m, is used in this equation rather than the potential between the cathode and the plasma, V_c. This is a direct consequence from the result that, as shown in the appendix, the average energy of those negative ions which have been retarded and reach the potential minimum in the sheath is the same as that of the total distribution leaving the cathode. As shown in figure 6, the negative ion density rises as the cathode is made more positive and the negative ion velocity is reduced. The point is reached when the presence of the virtual cathode starts to reduce the transmitted flux and the negative ion density decreases as the potential between the cathode and the plasma decreases and the depth of the virtual cathode increases.

Christ-Koch *et al* [22] measured the negative ion density in a caesiated source at a distance of 2.2 cm from the plasma grid using a laser photo-detachment method. This distance is approximately one hundred times the distance from the cathode to the sheath edge. Their results show a clear decrease in the negative ion density in the plasma as the plasma grid is biased increasingly positive with respect to the plasma. It has been pointed out by Bacal *et al* [23] that the decrease in the density of negative ions arising from the wall as the bias voltage (and hence their kinetic energy) is changed is not due to destruction of the negative ions by electron detachment, mutual neutralization or associative detachment. The mean free paths for these processes are much too long.

In the experiments of Christ-Koch *et al*, the whole plasma grid is biased with respect to the source body and hence effectively with respect to the plasma. As the plasma grid bias is increased the potential difference between the plasma and the grid decreases; at a bias voltage of 14 V the difference between the plasma potential and the bias potential is 2.2 V and at a bias voltage of 21 V this difference is zero. The plasma, at least in the extraction region, 'follows' the bias plate potential but these workers were able to operate at bias voltages of up to 24 V, i.e. with the plasma grid biased positively with respect to the plasma to some degree. At 3 V positive bias one would expect almost no negative ion flux from the wall yet in this experiment the extracted negative ion current only decreased slowly compared with the negative ion density. This has yet to be explained satisfactorily. When applying a positive bias to the cathode there was difficulty in finding a solution to Poisson's equation at large positive voltages. Small voltages could be used without difficulty, but voltages above ~1 V could only be used if the negative ion flux from the surface was higher than those realistically found. This is a result of a build-up of positive charge near the surface causing a maximum in the potential which the current model is insufficiently general to account for.

No account has been taken of secondary electron emission in the model. It has been shown that for positive biases secondary electrons can have an effect [24]. For materials such as caesium the secondary electron coefficient could be unity. Thus for an electron density of 4×10^{17} m^{-3} and a positive bias of 0.7 eV (equal to the estimated initial negative ion energy from the wall) the electron flux can be simply determined as ~31 000 A m^{-2}. Using the ratios of the electron and negative ion masses, this is an equivalent negative ion flux of 740 A m^{-2}. This is close to the estimated emitted negative ion flux and so would have an effect on the sheath and virtual cathode (which would be increased in depth). Thus for positive biases, the effect of secondary electrons should be considered.

4.3. Negative ion transport across the sheath as the negative ion density in the plasma is varied

The two examples given above of the application of the sheath model are more illustrative than realistic. Illustrative in the sense that it has been assumed that there are no negative ions in the plasma even though negative ions are being emitted at the cathode and reach the sheath edge. This is clearly not the case since the negative ions from the cathode will be accommodated in the plasma as the mean free path for their destruction is relatively long [23]. Furthermore negative ions are also produced in the plasma itself by dissociative attachment of electrons to vibrationally excited molecules.

The model has been used to investigate the effect of the presence of negative ions in the plasma. In this case the electron density at the sheath edge, n_{e0}, is 3.5×10^{17} m^{-3}, the electron temperature, T_e, is 2 eV, the positive ion and negative ion temperatures, T_i and T_n, are set at 0.8 eV, the emitted negative ion energy, $T_b/2$, is 0.7 eV and the cathode potential, $-V_c$, is −4 V. The emitted current density from the cathode is set at 600 A m^{-2}. The negative ion density, n_{n0}, at the sheath edge is then varied. The flux of negative ions at the sheath edge arising from the cathode is shown in figure 7 along with the depth of the virtual cathode as the ratio of negative ions to electrons at the sheath edge, n_{n0}/n_{e0}, is varied from 0 to 0.5. With no negative ions in the plasma the transported negative current density is 544 A m^{-2} with a virtual cathode depth of ~0.14 V. These values are the same as in figure 5 since this corresponds to the same conditions. As the relative density of the negative ions at the sheath edge is increased the transported current density increases to reach the emitted current density and the depth of the virtual cathode decreases to zero at a negative ion to electron ratio of ~0.21.

The increase in transported negative ion flux across the sheath from the cathode as the negative ion density in the

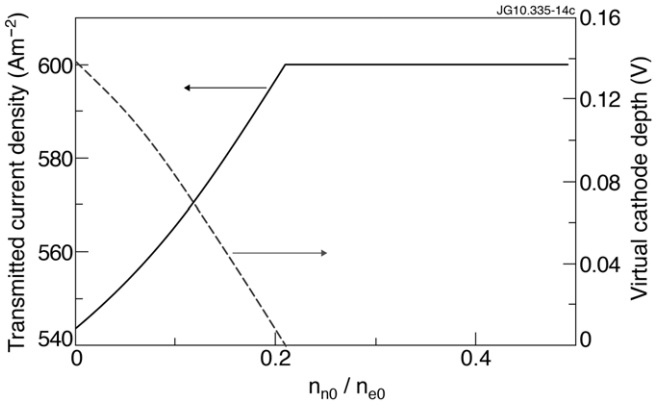

Figure 7. The negative ion current density (——) from the cathode arriving at the sheath edge and the virtual cathode depth (----) as the ratio of the densities of negative ions and electrons at the sheath edge relative is varied. The plasma conditions are given in the text.

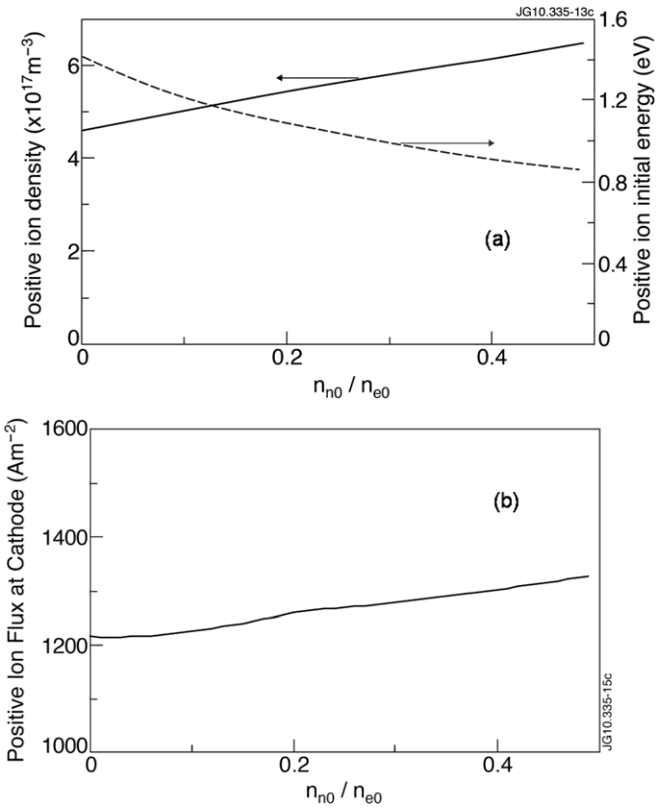

Figure 8. (*a*) The positive ion density (——) and initial energy (----) at the sheath edge and (*b*) the positive ion flux at the cathode as the ratio of the densities of negative ions and electrons at the sheath edge relative is varied. The plasma conditions are given in the text.

plasma increases can be understood from the charge neutrality requirement at the sheath edge. As the negative ion density in the plasma increases the negative space charge increases. To maintain neutrality the positive ion density must increase and thus the flux of positive ions in the sheath can increase. This allows a higher flux of negative ions from the cathode to balance the increased positive ion flux, as illustrated in figure 8.

Figure 8(*a*) shows the positive ion density, n_{i0}, at the sheath edge together with the initial energy, V_0, of the positive ions as they arrive at the sheath edge. The density increases to maintain neutrality and the initial energy of the positive ions falls. This fall in initial positive ion energy is in accordance with equations (13) and (14) where since j_b is relatively constant the behaviour is determined by the terms involving n_{n0}. In figure 8(*b*) the positive ion flux at the cathode is plotted showing that it is increasing thus allowing a higher negative ion flux from the cathode to balance the positive space charge.

5. Conclusion and future work

A 1D model of the sheath in a negative ion source relevant for future magnetic fusion heating beams has been developed. It is an extension of the work of Amemiya *et al* [10] taking into account the formation of a virtual cathode when the emitted negative flux from the cathode is greater than the space charge limit. The model is analytical and because it does not need to track millions of particles, a numerical solution to the model equations is found very quickly. The model has been used successfully to describe the conditions in the sheath for a wide range of example cases and has demonstrated good agreement with the PIC code of Wünderlich *et al* [9].

As input, the model requires two densities, such as the electron and negative ion densities, along with other parameters such as emitted current density and the particle temperatures, as used in the examples in section 4; the remaining density and transported beam flux are calculated. These densities are calculated at the sheath edge and not in the bulk plasma. This is the limitation of model as it currently stands when trying to compare with measurements: it is a model of the sheath and not of the sheath and the bulk plasma and densities at the sheath edge are not measured experimentally. One could assume a relationship between the density at the sheath edge and bulk plasma. For example if n_{ep} is the electron density in the plasma then it could be related to that at the sheath edge by $n_{ep} = n_{e0} \exp(U_0/T_e)$. The initial potential difference between the plasma and the sheath edge, U_0, is calculated from the model for known densities at the sheath edge. This relationship between the bulk plasma and the sheath edge could be incorporated into the convergence procedure to allow more detailed comparison with experimental data. This procedure has been carried out successfully [25] to compare the model with experimental measurements whereas the purpose of this paper has been to describe the sheath model in detail.

The way forward for the future development of this model is clear. In order to allow predictions for or comparisons with experiments the model needs to be combined with a model of the plasma. Such a model of a negative ion source has been described by Holmes [26]. This model uses moments of the Boltzmann equation to describe the plasma transport and takes into account the plasma collision processes associated with ionization and negative ion production and includes the magnetic field present in the source. It has been used successfully when compared with measurements from negative ion sources [26, 27] and in also describing species ratios in positive ion sources [28].

Despite the need to provide a self-consistent plasma model as input to this sheath model, the latter has already provided significant insight into the interaction between surface production of negative ions and the accompanying plasma, demonstrating a fundamental limit to the negative ion flux that can be transported into the plasma for extraction. This is particularly important in the search for materials to replace caesium in the role of promoting a low work function surface. In the presence of a virtual cathode, the density of negative ions measured in the plasma will be limited by the maximum transportable current density, regardless of the surface production rate. This could lead to 'false negative' results for candidate materials if researchers are not aware of the effect. Furthermore, this observation implies that efforts to increase the positive ion density would pay dividends if successful.

Acknowledgments

This work was funded by the RCUK Energy Programme under grant EP/I501045 and the European Communities under the contract of Association between EURATOM and CCFE. The views and opinions expressed herein do not necessarily reflect those of the European Commission.

Appendix

In order to determine the flux of negative ions transported across the sheath an initial energy for the negative ions is required. At the cathode this initial energy could be derived from an assumed temperature or directly calculated as shown by equations (1) and (7) in the main text. For the virtual cathode, the negative ions reaching the potential minimum will be retarded by the potential between the cathode and the virtual cathode. This appendix calculates a value for this average energy and gives the important result that the average energy at the virtual cathode is the same as that at the cathode. It is assumed that the negative ions emitted at the cathode have a Maxwellian distribution with temperature T_b (in electron volts) and thus energy in one dimension of $T_\mathrm{b}/2$. Then the one-dimensional Maxwellian velocity distribution is

$$f(v_x) = n\left(\frac{2M}{\pi e T_\mathrm{b}}\right)^{1/2} \exp\left(\frac{-Mv_x^2}{2eT_\mathrm{b}}\right) = C\exp\left(\frac{-Mv_x^2}{2eT_\mathrm{b}}\right) \tag{A1}$$

where $Mv_x^2/2e$ is the particle energy in electron volts. This distribution is normalized such that the integral between zero and infinity is n, the number of particles, i.e. only particles moving in the positive x-direction, are considered.

The average kinetic energy, $\overline{E}$, in the x-direction after crossing the retarding potential, V_k, is found by integrating the residual kinetic energy over the velocity distribution, f, with the velocity, u, at the potential, V_k, from zero to infinity by

$$\overline{E} = \frac{\displaystyle\int_0^\infty \frac{M}{2e}(v_x^2 - v_k^2) f(v_x)\,\mathrm{d}u}{\displaystyle\int_0^\infty f(v_x)\,\mathrm{d}u} \tag{A2}$$

where v_k is defined by

$$Mv_k^2 = 2eV_k \qquad \text{and} \qquad \frac{M}{2e}(v_x^2 - v_k^2) = \frac{Mu^2}{2e}.$$

The integral in the denominator of equation (A2) gives the fraction of the negative ions reaching the virtual cathode.

Multiplying the numerator and denominator by $\exp(Mv_\mathrm{k}^2/2eT_\mathrm{b})$ gives

$$\begin{aligned}\overline{E} &= \frac{M}{2e}\frac{\displaystyle\int_0^\infty u^2 \exp\left(-\frac{M}{2e}(v_x^2 - v_k^2)\right)\mathrm{d}u}{\displaystyle\int_0^\infty \exp\left(-\frac{M}{2e}(v_x^2 - v_k^2)\right)\mathrm{d}u} \\ &= \frac{M}{2e}\frac{\displaystyle\int_0^\infty u^2 \exp\left(-\frac{M}{2eT_\mathrm{b}}u^2\right)\mathrm{d}u}{\displaystyle\int_0^\infty \exp\left(-\frac{M}{2eT_\mathrm{b}}u^2\right)\mathrm{d}u}\end{aligned} \tag{A3}$$

and using standard integrals

$$\overline{E} = \frac{M}{2e}\frac{\frac{1}{4}\sqrt{\pi}(2eT_\mathrm{b}/M)^{3/2}}{\frac{1}{2}\sqrt{\pi}\sqrt{2eT_\mathrm{b}/M}} = \frac{T_\mathrm{b}}{2}. \tag{A4}$$

The mean kinetic energy in the x-direction is hence unchanged in going from the cathode surface to the virtual cathode for those ions whose initial energy is sufficient to overcome the potential barrier.

References

[1] ITER Design Description Document 5.3, N53 DDD 29 01-07-03 R0.1 2003 IAEA, Vienna
[2] Bacal M 2006 *Nucl. Fusion* **46** S250–9
[3] McAdams R, King R F, Proudfoot G and Holmes A J T 1992 *Production and Neutralisation of Negative Ions and Beams, 6th Int. Symp. 1992* ed J Alessi and A Herschovitch *AIP Conf. Proc.* **287** 353–67
[4] Fantz U *et al* 2007 *Plasma Phys. Control. Fusion* **49** B563–80
[5] Leung K N, Hauck C A, Kunkel W B and Walther S R 1989 *Rev. Sci. Instrum.* **60** 531–8
[6] Okumura Y, Hanada M, Inoue T, Kojima H, Matsuda Y, Ohara Y, Oohara Y, Seki M, Suzuki Y and Watanabe K 1990 *Proc. Symp. on Fusion Technology* (*London, UK, 1990*) pp 1026–30
[7] van Amersfoort P W, Geerlings J C C, Kwakman L F Tz, Hershcovitch A, Granneman E H A and Los J 1985 *J. Appl. Phys.* **58** 3566–72
[8] Takeiri Y *et al* 2010 *Rev. Sci. Instrum.* **81** 02B114
[9] Wünderlich D, Gutser R and Fantz U 2009 *Plasma Sources Sci. Technol.* **18** 045031
[10] Amemiya H, Annaratone B M and Allen J E 1998 *J. Plasma Phys.* **60** 81–93
[11] McAdams R and Bacal M 2010 *Plasma Sources Sci. Technol.* **19** 042001
[12] Hatayama A *et al* 2008 *Rev. Sci. Instrum.* **79** 02B901
[13] Taccogna A, Minelli P, Longo S, Capetelli M and Schneider R 2010 *Phys. Plasmas* **17** 063502
[14] McAdams R and Surrey E 2008 *1st Int. Symp. on Negative Ions Beams and Sources (Aix-en Provence, France 2008)* ed E Surrey and A Simonin *AIP Conf. Proc.* **1097** 89–98
[15] Seidl M, Cui H L, Isenberg J D, Kwon H J, Lee B S and Melnychuk S T 1996 *J. Appl. Phys.* **79** 2896–901

[16] Melnychuk S T, Seidl M, Carr W, Isenberg J and Lopes J 1989 *J. Vac. Sci. Technol.* A **7** 2127–31
[17] Lee B S and Seidl M 1992 *Appl. Phys. Lett.* **61** 2857–9
[18] Boyd R L F and Thompson J B 1959 *Proc. R. Soc. Lond.* **252** 102
[19] Braithwaite N St J and Allen J E 1988 *J. Phys. D: Appl. Phys.* **21** 1733
[20] Wünderlich D 2010 private communication
[21] Humphries S 1990 *Charged Particle Beams* (New York: Wiley)
[22] Christ-Koch S *et al* 2009 *Plasma Sources Sci. Technol.* **18** 025003
[23] Bacal M, McAdams R and Lepetit B 2010 *CCNB Meeting (Sofia, Bulgaria, May 2010)* unpublished
[24] Schiesko L, Carrère M, Cartry G and Layet J-M 2008 *Phys. Plasmas* **15** 073507
[25] McAdams R, King D B, Holmes A J T and Surrey E 2010 *2nd Int. Symp. on Negative Ions Beams and Sources (Takayama, Japan, 2010) AIP Conf. Proc.* in press
[26] Holmes A J T 1996 *Plasma Sources Sci. Technol.* **5** 453–73
[27] Al-Jibouri A, Holmes A J T and Graham W G 1996 *Plasma Sources Sci. Technol.* **5** 401–11
[28] King R F, Surrey E and Holmes A J T 2008 *Fusion Eng. Des.* **83** 1553–8